

pubs.acs.org/JPCA Perspective

Computational Modeling of the Conformation-Dependent Atmospheric Reactivity of Criegee Intermediates

Keith T. Kuwata*



Cite This: https://doi.org/10.1021/acs.jpca.4c04517



ACCESS I

Metrics & More

Article Recommendations

ABSTRACT: The impacts of Criegee intermediates (CIs) on atmospheric chemistry depend significantly on the CI conformation. In this Perspective, I highlight examples of how electronic structure and statistical rate theory calculations, in conjunction with experiment, have revealed conformation-dependent details of both CI ground-state reactivity and electronic excitation. Calculations using single-reference electronic structure methods and conventional transition state theory have predicted that CIs with *syn*-alkyl or *syn*-vinyl substituents isomerize rapidly to vinyl hydroperoxides (VHPs) or dioxoles, both of which can decompose rapidly under atmospheric conditions. Ongoing computational research on hydroxyl radical (OH) roaming initiated by VHP dissociation requires the application of multireference electronic structure methods and variational transition state theory. CIs that lack both *syn*-alkyl and

syn-vinyl substituents undergo either bimolecular reaction or $\pi^* \leftarrow \pi$ electronic excitation in the atmosphere. Accurate predictions of CI ultraviolet—visible spectra require multireference calculations with large active spaces and at least a second-order perturbative treatment of dynamic electron correlation. The extent to which electronic spectra can be diagnostic of the presence of specific CI conformers varies significantly with CI chemical identity.

I. INTRODUCTION

In the atmosphere, alkene ozonolysis produces Criegee intermediates (CIs). Since the 1990s, computation—in particular, electronic structure and statistical rate theory calculations—has played a critical role in revealing how CI reactivity on the electronic ground state depends on conformation. Computation has also identified CI conformers whose unimolecular and bimolecular reactivities are both slow enough to make electronic excitation and photochemistry their dominant atmospheric fate. In this Perspective, I describe both historical and recent insights yielded from computation, discuss both agreements and disagreements with experiment, and identify current methodological challenges.

II. CONFORMATIONAL DEPENDENCE OF GROUND-STATE CRIEGEE INTERMEDIATE REACTIVITY

II.A. OH Production from *Syn*-Alkyl Cls. My consideration of conformation-dependent reactivity starts with the smallest substituted CI, acetaldehyde oxide, CH₃CHOO. Scheme 1 presents the dichotomy in reactivity for the *syn* (1) and *anti* (6) conformers of CH₃CHOO.

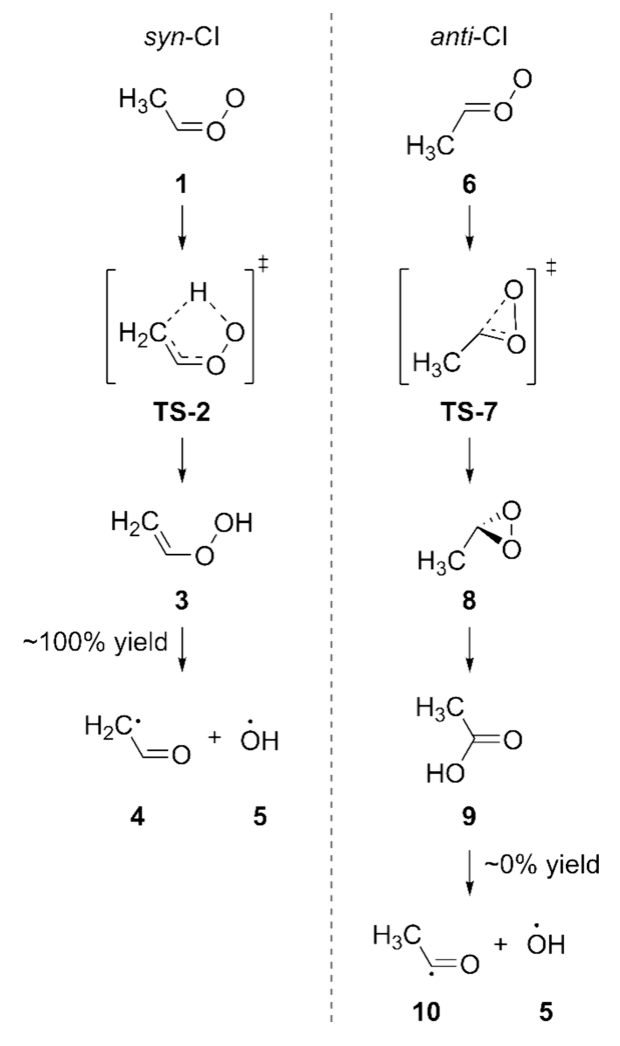
Seminal quantum chemical studies in 1996 by Gutbrod et al. and Anglada et al. predicted that, with respect to unimolecular reactivity, CIs with an alkyl group *syn* to the peroxy bond (e.g., 1) preferentially undergo an intramolecular 1,4-hydrogen shift

(via TS-2) to form vinyl hydroperoxides (VHPs, 3) that often quantitatively decompose to afford vinoxy and hydroxyl (OH) radicals (4 + 5). (We will consider an alternative VHP reaction pathways in Section IID below.) In contrast, formaldehyde oxide (CH₂OO) and CIs with alkyl groups only anti to the peroxy bond (e.g., 6) preferentially cyclize (via TS-7) to dioxiranes (8). Early CCSD(T) and MR-AQCC calculations by Cremer et al.⁴ predicted that 8, in turn, largely isomerizes to carboxylic acids (9) via open-shell diradical intermediates (not shown). Early work by Kroll et al.5 attributed the ~15% yield of OH from ethene ozonolysis, which can generate only the parent CI, CH₂OO, to the decomposition of chemically activated 9 to 10 + 5. However, more recent work by Nguyen et al. employing the HEAT-345(Q) quantum chemical method and a two-dimensional (energy and angular momentum) master equation simulation attributed virtually all of the OH from ethene ozonolysis to decomposition of primary ozonide diradical intermediates (not shown).

Received: July 5, 2024
Revised: August 13, 2024
Accepted: August 16, 2024



Scheme 1. Unimolecular Reactivity of syn-Methyl and anti-Methyl Criegee Intermediates^a



^aAdapted from ref 24. Copyright 2010 American Chemical Society.

Given that OH is the most important oxidant in the troposphere, the predicted conformational dependence of CI reactivity has high atmospheric significance. Conformation-specific CI syntheses, coupled with infrared (IR) CI excitation and ultraviolet (UV) OH detection, by Liu et al., Lu et al., and Fang et al. La, have provided direct experimental confirmation of the predictions of significant OH production from *syn*-alkyl CI.

Predicting the atmospheric impact of CIs based solely on conformation-dependent unimolecular reactivity suffices for the fraction of CI that is formed chemically activated via alkene ozonolysis. However, as predicted back in 2001 by Kroll et al., 14 a significant fraction of even small CIs (i.e., CIs containing four or fewer carbon atoms) is either formed vibrationally "cold" or experiences collisional stabilization under atmospheric conditions. These stabilized CI (SCI) are susceptible to bimolecular reactions in the atmosphere, particularly with water $^{15-17}$ and sulfur dioxide. $^{18-21}$ In this Perspective, I will focus on the water reaction. In 2003, Hasson et al. 22 provided both experimental and theoretical evidence that the α -hydroxy hydroperoxide (14, Scheme 2) formed in the SCI + $\rm H_2O$ reaction does not decompose to afford OH.

Scheme 2. Bimolecular Reactions of Stabilized syn and anti Criegee Intermediates with Water Monomer^{a,b}

"Numbers in blue are IUPAC-recommended second-order rate constants (cm³ molecule⁻¹ s⁻¹) at 298 K from Cox et al.²³ ^bAdapted from ref 24. Copyright 2010 American Chemical Society.

Thus, determining the relative rates of the unimolecular 1,4-hydrogen shift reaction and the bimolecular hydration reaction of *syn*-alkyl CI is critical for assessing the atmospheric impact of SCIs. In 2010, Kuwata et al.²⁴ predicted that the *syn*-methyl SCIs 1, 16a, and 16b (Scheme 3) formed in *trans*-2-butene ozonolysis

Scheme 3. *syn*-Methyl-Stabilized Criegee Intermediates Studied by Kuwata et al.²⁴

$$H_3C = 0$$
 $H_3C = 0$ $H_3C = 0$ $H_3C = 0$ $H_3C = 0$

(in the case of 1) and isoprene (2-methyl-1,3-butadiene) ozonolysis (in the case of 16a and 16b) will isomerize and decompose to OH faster than the SCIs will react with water at typical atmospheric temperatures and H_2O concentrations; that is, the OH yields from *trans*-2-butene and isoprene ozonolysis should not depend on relative humidity in the atmosphere.

Subsequent conformer-specific CI hydration kinetics measurements by Taatjes et al., ²⁵ experimental and modeling studies by Novelli et al., ²⁶ and highly accurate electronic structure and transition state theory (TST) calculations by Long et al. ²⁷ largely substantiated the prediction that OH production from *syn*-CH₃CHOO is unaffected by the water reaction. More recent

Scheme 4. Fastest Unimolecular Reactions for the Four Conformers of Methyl Vinyl Ketone Oxide Produced in Isoprene Ozonolysis a,b

"Numbers in green are CBS-QB3 zero-point-corrected electronic energies (kcal mol⁻¹), all relative to the energy of **16a**, from Kuwata et al. Numbers in blue are first-order transition state theory rate constants (s⁻¹) at 298 K calculated for this article using CBS-QB3 energies, B3LYP/6-311(2d,d,p) partition functions, and the Eckart tunneling method. Adapted from ref 39. Copyright 2005 American Chemical Society.

experimental work by Robinson et al. ²⁸ confirmed that isomerization of syn-CH₃CHOO via a 1,4-hydrogen shift, with a 298 K rate constant of \sim 150 s⁻¹, will be faster than its reaction with water monomer and SO₂ under atmospheric conditions; with concentrations of [H₂O] and [SO₂] typical of the lower troposphere, ²³ the pseudo-first-order rate constants are $<60 \text{ s}^{-1}$ and \sim 0.65 s⁻¹, respectively. Master equation modeling by Robinson et al. ²⁸ performed with the MESMER code ²⁹ predicted that, were it not for hydrogen-atom tunneling, the 1,4-hydrogen shift rate constant would be only \sim 5 s⁻¹ at 298 K. Since we still do not have an experimental value for the rate constant of the syn-CH₃CHOO + (H₂O)₂ reaction, we cannot exclude the possibility that the water dimer reaction could measurably decrease OH yield under certain atmospheric conditions, as previously noted by Novelli et al. ²⁶

Work published since the 2010 Kuwata study²⁴ has also confirmed the contention that the production of OH from isoprene-derived syn-methyl CI will not be affected by relative humidity. Using structure-activity relationships, Vereecken et al. 30 estimated that syn-methyl vinyl ketone (MVK) oxide (16a and 16b, Scheme 3) has a unimolecular rate constant ~1000 times greater than this CI's pseudo-first-order rate constant with respect to water monomer and dimer in the troposphere, making both chemically activated and stabilized syn-methyl vinyl ketone oxide potentially substantial tropospheric OH sources. Subsequent work supported Vereecken et al.'s predictions: Barber et al.³¹ combined IR action spectroscopy and RRKM/master equation simulations to determine that syn-MVK oxide has a unimolecular decay rate of 33 s⁻¹. Caravan et al.³² used direct UV-visible absorption spectroscopy to determine an upper limit for the syn-MVK oxide + H₂O reaction rate constant of 4.0 \times 10⁻¹⁷ cm³ molecule⁻¹ s⁻¹, leading to a pseudo-first-order rate constant of $<10 \text{ s}^{-1}$. With respect to the atmospheric fate of syn-MVK oxide, it is important to note that its unimolecular loss rate is ~5 times slower than that of syn-CH₃CHOO, making syn-MVK oxide more prone to photodissociation than syn-CH₃CHOO, as noted by Caravan et al.³² This would attenuate

the OH yield from *syn*-MVK oxide. We will consider the electronic excitation of MVK oxide in Section IIIC below.

II.B. Cyclization and Hydration Reactions of anti-Alkyl Cls. The atmospheric chemistry of anti-CI is fundamentally different from that of syn-CI. First, the anti conformers react much faster with water. Multiple quantum chemical studies using CCSD(T) theory with triple- ζ basis sets^{33–35} and the MCG3 method²⁴ (a QCISD(T)-based composite method designed by Lynch and Truhlar³⁶) all predicted an activation barrier for the anti-CH₃CHOO + H₂O reaction 6-7 kcal mol⁻¹ lower in energy than the barrier for the syn-CH₃CHOO + H₂O reaction. Kuwata et al.²⁴ attributed this difference in barrier heights both to the lower steric hindrance against the approach of the H₂O to anti-CH₃CHOO and to the loss of homoaromatic stabilization in syn-CH₃CHOO^{37,38} as the syn conformer distorts from planarity to interact with H₂O. This barrier height difference is the main reason that anti-CI reacts several orders of magnitude faster with water than does syn CI (see Scheme 2 above). Based on an extensive structure-activity relationship analysis, Vereecken et al.³⁰ concluded that, for typical alkyl substituents, the loss of anti-CI in the atmosphere due to dioxirane formation (Scheme 1 above) has a rate constant of \sim 50 s⁻¹, while atmospheric loss of anti-CI due to reaction with water monomer has a pseudo-first-order rate constant of ~7000 s⁻¹. Thus, CIs with a *syn*-hydrogen and an *anti*-alkyl substituent will not be a significant source of carboxylic acid (via dioxirane) in the atmosphere.

Scheme 4 presents the fastest unimolecular reaction pathway for each of the four conformers of MVK oxide. The atmospheric fate of *anti*-methyl MVK oxide (conformers **16c** and **16d**) is fundamentally different from the fate of *anti*-CH₃CHOO due to the presence in **16c** and **16d** of a *syn*-vinyl group. As first predicted by Kuwata et al.³⁹ on the basis of CBS-QB3 calculations (energies in Scheme 4), the lowest-barrier isomerization process for MVK oxide is a 1,5-electrocyclization (via **TS-21d**) to dioxole (**22d**), with a activation barrier of only 11.0 kcal mol⁻¹ with respect to the *anti-cis* CI conformer (**16d**). Kuwata et al. also reported RRKM/master equation simulations

Scheme 5. Fastest Unimolecular Reactions for the Four Conformers of Methacrolein Oxide Produced in Isoprene Ozonolysis a,b

"Numbers in green are CBS-QB3 zero-point-corrected electronic energies (kcal mol⁻¹), all relative to the energy of **23c**, from Kuwata and Valin. Numbers in blue are first-order transition state theory rate constants (s⁻¹) at 298 K calculated for this article using CBS-QB3 energies, B3LYP/6-311(2d,d,p) partition functions, and the Eckart tunneling method. Adapted with permission from ref 46. Copyright 2008 Elsevier.

Scheme 6. Eight Conformers of 2-Butenal Oxide a,b,c

^aThe three-character stereochemical labels indicate the following: The first character indicates if the C=C and C=O bonds are *cis* or *trans*. The second character indicates if the geometry around the C=O bond is E or E. The third character indicates if the geometry around the C=C bond is E or E. Numbers in green are CCSD(T)-F12b/cc-pVTZ-F12//B2PLYP-D3/cc-pVTZ zero-point-corrected electronic energies (kcal mol⁻¹), all relative to the energy of 28-cZE, from Hansen et al. Adapted from ref 47. Copyright 2022 American Chemical Society.

(using Barker's MultiWell code ^{40,41}) of the chemically activated fraction of MVK oxide formed in isoprene ozonolysis. These simulations indicated that the barrier for rotation of the vinyl group in the *anti*-methyl MVK oxide (~8 kcal mol⁻¹ according to CBS-QB3) is low enough for virtually all of the chemically activated *anti-trans* conformer (16c) to convert to the *anti-cis* conformer (16d) and then cyclize irreversibly to 22d. Thus, formation of dioxirane 20c is negligible. More recent computational work by Barber et al. ³¹ confirmed the kinetic favorability of dioxole formation, predicting a barrier for Reaction 4 (Scheme 4) of 15.06 kcal mol⁻¹ using the highly accurate ANL0-B2F composite method. ⁴² Barber et al. also predicted the

existence of a number of radical-forming decomposition pathways for the chemically activated dioxole, pathways that were confirmed in multiplexed photoionization mass spectrometric (MPIMS) measurements by Vansco et al. In sum, the major atmospheric fate of *anti-MVK* oxide is unimolecular isomerization and decomposition, not photodissociation. In contrast, *syn-MVK* oxide conformers isomerize 3 orders of magnitude slower than the *anti* conformers, making electronic excitation and photodissociation of the *syn* conformers a major atmospheric fate. 2

The MVK oxides discussed thus far arise from addition of O_3 to the isoprene 1,2-double bond. Addition of O_3 to the isoprene

3,4-double bond produces methacrolein (MACR) oxide (conformers 23a, 23b, 23c, and 23d in Scheme 5). Scheme 5 shows the fastest unimolecular reaction pathway available to each of the four MACR oxide conformers. Unlike MVK oxide, none of the MACR oxide conformers is capable of a 1,4hydrogen shift leading to a VHP; the only low-barrier pathways are formation of dioxole 25a (via TS-24a) and formation of dioxirane conformers 27b and 27d (via TS-26b, TS-26c, and TS-26d). In 2008, Kuwata and Valin⁴⁶ reported the CBS-QB3 energies shown in Scheme 5, predicting that Reaction 5, dioxole formation, has a barrier of only 11.9 kcal mol⁻¹.

Kuwata and Valin⁴⁶ used MultiWell^{40,41} to perform RRKM/ master equation simulations of the chemically activated MACR oxides formed in isoprene ozonolysis. At 1 atm pressure, all of the chemically activated syn conformers (23a and 23b) formed dioxole 25a, indicating facile conversion of the syn-trans CI to the syn-cis conformer. More recently, Vansco et al. 44 provided experimental confirmation of the kinetic favorability of the dioxole pathway, reporting the detection via MPIMS⁴³ of multiple species derived from the decomposition of 25a. The TST first-order rate constants noted in Scheme 5 show that the anti-MACR oxide conformers isomerize roughly 3 orders of magnitude slower than the syn-cis conformer. Thus, we expect electronic excitation and subsequent photochemistry to play much larger roles in determining the atmospheric fate of the anti-MVK oxide conformers.

As presented above, the synergy of theory and experiment has provided a rigorous and conformer-specific understanding of the unimolecular and bimolecular chemistry of MVK oxide and MACR oxide. One outstanding challenge is to achieve the same level of chemical understanding for CIs with even more conformational forms. In this regard, a logical system to

II.C. Ongoing Challenges: Multiple CI Conformations.

consider is the structural isomer of MVK oxide and MACR oxide; namely, 2-butenal oxide, which possesses eight conformers. Scheme 6 presents these conformers along with their stereochemical labeling and relative stabilities as reported by Hansen et al.47

With the increase in conformational complexity also comes a new reactive pathway arising from the presence of C-H bonds in 28 that are both allylic to the C=C bonds and gamma to the carbonyl oxide C. Specifically, Vereecken et al. 30,48 predicted that structures like 28-cZZ can undergo a rapid 1,6-hydrogen shift (via TS-29 in Scheme 7) to form a VHP (30). Vereecken et al. estimated the hydrogen-shift barrier in syn-2-butenal oxide (28-cZZ) to be 8.5 kcal mol⁻¹ lower in energy than the hydrogen-shift barrier in syn-acetaldehyde oxide (1). Compared to the five-membered ring of TS-2, the seven-membered ring of TS-29 has much less ring strain and a nearly linear C--H--O bond angle. 49 The dramatically lower activation barrier leads to a thermal (298 K) rate constant for the 1,6-hydrogen shift of 28cZZ that is 4 orders of magnitude higher than for the 1,4hydrogen shift of 1. This, in turn, leads to a predicted rapid formation of OH (5) along with the vinoxy radical coproduct (31).

Hansen et al.⁴⁷ provided both explicit experimental confirmation of, and conformational specificity to, the predicted 1,6-allylic hydrogen shift. Using a combination of isomerspecific synthesis, IR excitation of the 2-butenal oxide C-H stretches, and time-dependent UV detection of OH, in conjunction with high-level ANLO-B2F calculations, 42 the authors determined that OH formation is triggered by excitation of the more stable (see Scheme 6 above) 28-tZZ conformer; the

Scheme 7. Intramolecular H-Atom Abstractions from an Alkyl vs an Allyl Group

^aNumbers in green are CCSD(T)//M06-2X/aug-cc-pVTZ zeropoint-corrected reaction barriers (kcal mol^{-1}), both with a + 0.4 kcal mol⁻¹ correction, from Vereecken et al.³⁰ Numbers in blue are firstorder transition state theory rate constants (s⁻¹) at 298 K calculated using the barriers in green, M06-2X/aug-cc-pVTZ partition functions, and the Eckart tunneling method.45

excitation allows it to interconvert to 28-cZZ, which has the requisite geometry to undergo the 1,6-hydrogen shift. The ANL0-B2F energetics, combined with the use of the Master Equation System Solver (MESS) code, 50 leads to an effective thermal rate constant for OH formation from 2-butenal oxide (via the pathway in Scheme 7) of 8×10^5 s⁻¹ at 298 K. Thus, under atmospheric conditions, the lifetimes of the 28-cZZ and the 28-tZZ conformers should be extremely short. Moreover, based on the 2-butenal oxide energetics reported by Hansen et al., 47 and in analogy with MVK oxide and MACR oxide results considered above, we would also anticipate short lifetimes for the 28-tZE and the 28-cZE conformers. This is because 28-cZE can rapidly cyclize to a chemically unstable dioxole and there is a modest barrier for the interconversion of 28-tZE and 28-cZE. Therefore, we would expect UV-visible excitation and photodissociation to dominate the atmospheric fates of the less reactive *anti* conformers (28-cEZ, 28-tEZ, 28-tEE, and 28-cEE).

Scheme 8. Criegee Intermediates Generated in α -Pinene Ozonolysis

Scheme 9. Unimolecular Reactions of the 1-Methyl Vinyl Hydroperoxide with Roaming Transition Structures in Red^{a,b}

^aNumbers in green are zero-point-corrected energies (kcal mol⁻¹), relative to the combined energies of **44** and **5**, based either on EOM-SF-CCSD(dT) theory^{69,70} with the cc-pVTZ basis set (for open-shell-singlet species) or W1BD theory⁷¹ (for all other species) from Kuwata et al.⁶⁸ Adapted from ref 68. Copyright 2018 American Chemical Society.

2-Butenal oxide is perhaps the largest CI for which it is reasonable to locate and optimize all conformers manually. Calculations on larger CIs, such as those formed in the ozonolysis of the atmospherically abundant α -pinene^{51,52} (34a, 34b, 34c, and 34d in Scheme 8), almost necessarily require some automatic generation of conformers. Studying CIs of this size and conformational complexity is necessary to gain a better understanding of the formation of atmospheric aerosols, ⁵³ which have large impacts on climate ⁵⁴ and human health. ⁵⁵

A noteworthy conformational-searching approach by the Kurtén laboratory is to use either the molecular mechanics engine in Spartan or the semiempirical tight-binding methods in CREST to generate all possible conformers of a covalently bonded framework, optimize all of these conformers with an inexpensive density functional theory (DFT) model chemistry, and then reoptimize a subset of the DFT-optimized structures within a certain energy of the ground-state conformer with a more accurate model chemistry. One can treat transition structures and noncovalent complexes with the same approach by performing the initial screening with appropriately frozen atom—atom distances. This automated approach has been

successful in modeling experimental results from studies of the formation of highly oxygenated molecules in α -pinene ozonolysis⁵⁹ and the reaction of isoprene and terpenes (all with molecular formula $C_{10}H_{16}$) with acylperoxy radicals.⁶⁰

II.D. Ongoing Challenges: Dissociation vs Roaming of the OH from the VHP. Theoretical treatments of the unimolecular and bimolecular reactions of the smaller CIs discussed in sections IIA and IIB have been methodologically accessible in that the use of single-reference electronic structure methods (with extrapolations to complete-basis-set limits), RRKM theory for calculating microcanonical rate constants, and the simple Eckart method to model tunneling have produced predictions in excellent agreement with experiment. However, more technically demanding multireference electronic structure and variational TST methods are proving necessary for the accurate modeling of the unimolecular reactivity of VHPs.

For decades, there has been experimental evidence suggesting that some fraction of the VHP formed in alkene ozonolysis rearranges to a hydroxycarbonyl under certain conditions. ^{61–64} Definitive observation by Taatjes et al. ⁶⁵ of hydroxyacetone formation from the dimethyl CI (43 in Scheme 9) along with

theoretical insights from Kurtén and Donahue, ⁶⁶ Kidwell et al., ⁶⁷ and Kuwata et al., ⁶⁸ established the key mechanistic features of unimolecular VHP (37a and 37b) reactivity, as shown in Scheme 9.

Consistent with the definition of roaming by Suits, ⁷² in the VHP system, the dissociation of the OH radical is "frustrated" by its attraction to the vinoxy radical (44), resulting in shallow radical pair minima 40a and 40b. The long-range nature of the radical—radical interaction gives the OH freedom to roam along a flat potential either between different conformers of the radical pair (via TS-41) or toward the other radical center (via TS-42a) to form hydroxyacetone (43). The atmospheric significance of roaming is that it has the potential to reduce the OH yield from *syn*-alkyl CIs. Roaming is not strictly confined to the minimum energy path defined by the submerged (relative to free vinoxy and OH radicals) saddle points TS-41 and TS-42a, but, as rigorously demonstrated by Klippenstein et al., ⁷³ a statistical model of roaming can predict branching fractions in excellent agreement with trajectory-based simulations.

In their 2018 study, Kuwata et al.⁶⁸ performed statistical rate theory simulations of the mechanism in Scheme 9 for both chemically activated and thermalized 35. MultiWell^{40,74} simulations of chemically activated 35 predicted only two possible outcomes: dissociation to 44 + 5 or collisional stabilization of 35. In contrast, MESMER²⁹ simulations of thermalized 35 predicted not only dissociation to 44 + 5, but also formation of 43 and temporary accumulation of the VHP (37a + 37b); branching to the latter two outcomes increased with decreasing temperature.

More recently, the Klippenstein laboratory has provided detailed theoretical descriptions of roaming in the vinoxy–OH systems derived from MVK oxide,³¹ the methyl–ethyl CI,^{75,76} and the CIs formed in a-pinene ozonolysis.⁷⁷ These studies, which focus on VHPs formed from thermalized CIs, illustrate state-of-the-art approaches in computational treatments of VHP roaming.

The first methodological challenge is the participation of numerous open-shell-singlet (OSS) species (e.g., TS-39a, TS-39b, 40a, 40b, TS-41, and TS-42a in Scheme 9 above) whose electronic structure can be significantly multireference in character. Klippenstein's approach is to apply a high-level, but nevertheless single-reference, electronic structure method such as CCSD(T)-F12 to all species in the mechanism, treating each OSS as a triplet (obtaining energy ${}^{3}E$). The next step is to use a multireference method to calculate the singlet-triplet energy gap (obtaining energy ΔE_{S-T}) for each OSS species. One then obtains an accurate estimate for the OSS energy with the expression $E(OSS) = {}^{3}E + \Delta E_{S-T}$. The virtue of this approach is that, as demonstrated by Pfeifle et al., 78 one can use a significantly lower level of multireference electronic structure theory to predict an accurate ΔE_{S-T} than one would need to use if he were computing E(OSS) directly. The study of VHPs formed from the methyl-ethyl CI⁷⁵ confirms the same methodological finding: using a (3,3) active space and extrapolations to the complete-basis-set limit, the mean average deviation between CASPT2 and the MRCI+Q predictions of $\Delta E_{\text{S-T}}$ is only 0.14 kcal mol⁻¹. Being able to use a multireference method with a lower level of dynamic electron correlation like CASPT2 has made possible Klippenstein and Elliott's 77 accurate modeling of the C_{10} VHPs derived from α -pinene ozonolysis.

The second methodological challenge is the accurate treatment of roaming kinetics. There are multiple loose transition states in the roaming region of the potential energy surface and there is still ambiguity about the choice of statistical model. The Klippenstein laboratory uses variable reaction coordinate-transition state theory (VRC-TST)^{79,80} for loose transition states in conjunction with the MESS master equation code,⁵⁰ which automatically invokes the statistical model of roaming formulated by Klippenstein et al.⁷³ The methyl—ethyl CI study by Liu et al.⁷⁵ does an excellent job of illustrating how predicted branching fractions depend on assumptions about the relative rates of dissociation on the ground state vs coupling of ground and excited electronic states as well as whether or not to assume rapid roaming; that is, instantaneous equilibrium of different radical pair conformers. Another practical option for treating loose transition states is the ktools variational transition state theory code incorporated into Barker's MultiWell master equation package. ^{40,82}

III. RECENT COMPUTATIONAL STUDIES OF CRIEGEE INTERMEDIATE ELECTRONIC EXCITATION

III.A. Benchmarking against the Parent CI Experimental Spectrum. Thanks to the synergy of experiment and theory, we now have a firm understanding of the impact of conformation on (smaller) CI unimolecular and bimolecular reactivity in the ground electronic state. It is therefore appropriate now for theorists to focus more on the role of electronic excited states in determining the atmospheric fate of CIs. Guided by experiment, theorists have been seeking to capture the conformational dependence of the UV-visible absorption spectrum and photodissociation to carbonyl and O atom moieties caused principally by excitation to the B^1A' state, a $\pi^* \leftarrow \pi$ transition that dissociates the Criegee's O-O bond. 83 In this Perspective, I will restrict my discussion to predictions of absorption spectra. I focus on recent work by Nikoobakht and Karsili, starting with their treatments of the UV-visible spectrum of the smallest CI, CH2OO, and then describing how they extend their methodologies to larger CIs that can adopt more than one conformer.

Nikoobakht has published several computational studies of CI UV-visible spectroscopy. In their 2021 study of CH₂OO, Nikoobakht and Köppel⁸⁴ posited four keys to accurate modeling of CI electronic spectroscopy and excited state dynamics: (1) using an electronic structure method that explicitly treats both static and dynamic electron correlation, (2) a quantum-mechanical treatment of wavepacket dynamics, (3) quantifying how CI UV-visible spectra depend significantly on wavepacket dynamics along more than the O-O dissociation coordinate (R(O-O)), and (4) treating more than the ground $X^{1}A'$ and the $B^{1}A'$ excited electronic state. Specifically, in modeling CH2OO, Nikoobakht and Köppel used the MRCI+Q-F12b(18,14)/aug-cc-pVTZ (and the EOM-CCSD/aug-ccpVTZ) model chemistries to compute electronic excited state potentials, the Multi-Configuration Time Dependent Hartree (MCTDH) approach⁸⁵ to describe wavepacket propagation, computed electronic structure and dynamics as a function of both R(O-O) and the C-O-O bond angle $(\theta(C-O-O))$, and treated coupling between the B^1A' and C^1A' electronic excited states. The active space used in their MRCI calculations comprised all of the valence electrons and orbitals in CH₂OO. A subsequent study of CH₂OO by Nikoobakht and Köppel⁸⁶ tested a explicitly correlated multireference method, CASPT2-F12, that, unlike MRCI+Q-F12b, treats dynamic electron correlation only to second order.⁸⁷ This follow-up study also incorporated three CH_2OO internal coordinates: R(O-O), $\theta(C-O-O)$, and the C-O distance, R(C-O).

The Journal of Physical Chemistry A

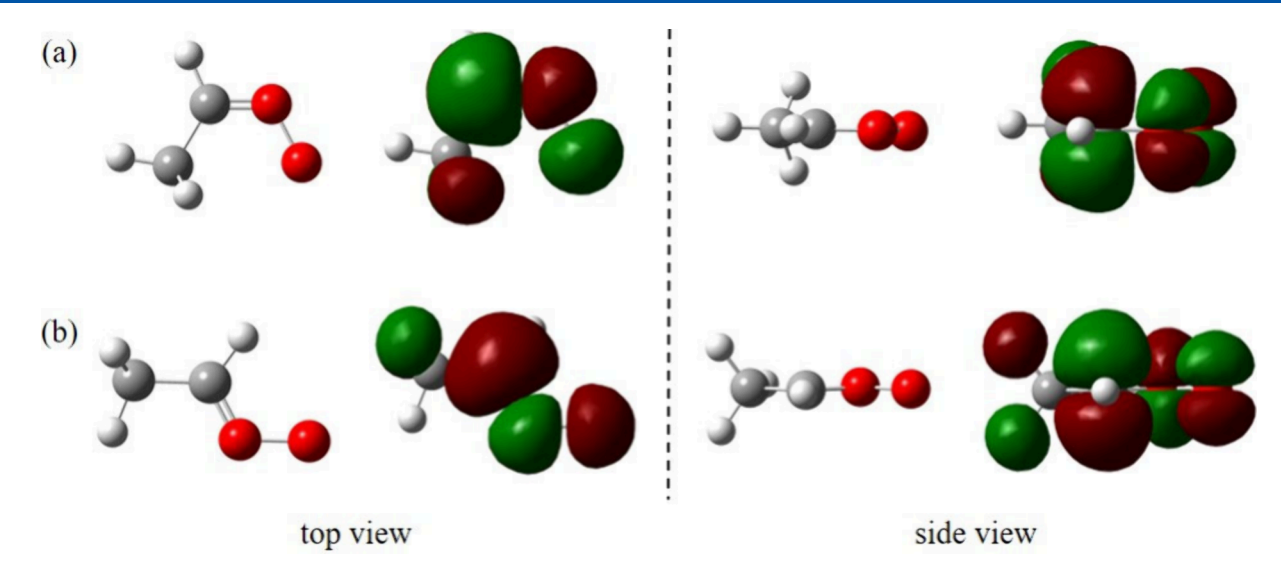


Figure 1. Top and side views of the π^* molecular orbital populated upon UV excitation of the (a) *syn* and (b) *anti* conformers of CH₃CHOO. Note that the *syn* conformer has a through-space π^* interaction between the terminal O and the out-of-plane methyl Hs, while the *anti* conformer lacks this destabilizing interaction. The probability contours shown are from HF/STO-3G calculations conducted by the author.

Karsili and co-workers have also published several computational studies of Criegee intermediate UV-visible spectroscopy, taking a more affordable approach than that of Nikoobakht and Köppel. In their 2021 study of CH2OO, McCoy, Marchetti, Thodika, and Karsili (McCoy et al. 88) proposed the following methodology: (1) using lower levels of ab initio theory than MRCI+Q along with calibrated variants of time-dependent density functional theory (TDDFT), (2) eschewing an explicit quantum-mechanical treatment of dynamics, and (3) sampling a large set of distortions of the ground-state equilibrium geometry via a nuclear ensemble method. Specifically, McCoy et al. 88 tested CASPT2-F12/aug-cc-pVDZ with (12,10) and (10,8) active spaces; they also tested TDDFT with the ω B97X-D and CAM-B3LYP functionals and the 6-311+G(d,p) basis set. McCoy et al. used these electronic structure methods to calculate the excitation energies and transition dipoles for a Wigner distribution of ground-state geometries⁸⁹ (i.e., distorting the ground state equilibrium geometry along all 3N - 6 normal modes). The CASPT2 active spaces used by McCoy et al. were both smaller than that used by Nikoobakht and Köppel.⁸⁴

Overall, both Nikoobakht and Köppel⁸⁴ and McCoy et al.⁸⁸ successfully reproduced the experimental UV-visible absorption spectrum of CH₂OO as reported by Beames et al., Sheps, ⁹¹ Ting et al., ⁹² and Foreman et al. ⁹³ In the Nikoobakht and Köppel work, the MRCI+Q vertical excitation energy (3.75 to 3.83 eV, depending on the active space) and peak width (\sim 70 nm full-width at half-maximum) agree best with the measurements of Beames et al.⁹⁰ The EOM-CCSD vertical excitation energy of 4.01 eV is significantly higher than experiment, 90-92 which suggests that an explicit treatment of static electron correlation, which is missing from EOM-CCSD theory, is necessary for quantitative accuracy. With respect to dynamics, Nikoobakht and Köppel acknowledged that the simpler treatment of Dawes et al.⁹⁴ also agreed well with experiment. (Dawes et al. predicted the CH₂OO UV-visible spectrum based upon Heller's short-time-scale excited wavepacket propagation on the adiabatic B-state potential energy surface, which is highly repulsive in the Franck-Condon region.) Like Nikoobakht and Köppel,84 McCoy et al.88 also achieved the best agreement with the experimental vertical excitation energy of Beames et al.; 90 the agreement with the peak width of Beames et al. is a somewhat fortuitous consequence of an arbitrarily chosen broadening factor. The CASPT2(12,10) predictions agreed with experiment slightly better than CASPT2(10,8) and MRCI(10,8), which suggests that a more complete treatment of static electron correlation, achieved with a larger active space, is more important for quantitative accuracy than the level of treatment of dynamic electron correlation, which is greater for MRCI than for CASPT2.⁹⁶ (However, at least some treatment of dynamic electron correlation greatly enhances the accuracy of predicted excitation energies, as demonstrated by CASSCF vs. MRCI+Q calculations for the $\pi^* \leftarrow \pi$ transition in CH₂OO by Takahashi. The wavelength of maximum absorbance (λ_{max}) values for the ω B97X-D and CAM-B3LYP spectra were both at ${\sim}275$ nm, ${\sim}75$ nm to the blue of the experimental $\lambda_{\rm max}$ values. Thus, shifting the TDDFT spectra ~0.7 eV to the red brought them into agreement with experiment.

The most obvious difference in the Nikoobakht and Köppel^{84,86} and McCoy et al.⁸⁸ predictions was the treatment of vibrational structure in the low-energy side of the peak observed by Sheps,⁹¹ Ting et al.,⁹² and Foreman et al.⁹³ Nikoobakht and Köppel predicted vibrational progressions due both to the O-O stretching and the C-O-O bending modes of roughly the same spacing as experiment (\sim 0.08 eV and \sim 0.07 eV, respectively). They attributed the vibrational structure to the reflection of the wavepacket at the barrier created by the avoided crossing (at $R(O-O) \approx 2.1 \text{ Å}$) between the B and C states. A one-dimensional model based only on R(O-O) accurately predicted the locations of the observed vibrational peaks, while inclusion of the $\theta(C-O-O)$ and R(C-O) coordinates predicted fine spectral features not currently resolvable by experiment. It is also noteworthy that the vibrational features predicted using CASPT2-F12 theory agreed far better with experiment that the features predicted by MRCI+Q-F12b theory. The nuclear ensemble method used by McCoy et al. cannot reproduce the observational vibrational structure, but the authors contended that the computational efficency of the method, if coupled with a highly accurate or calibrated electronic structure method, can predict peak locations and photoabsorption cross sections accurate enough to guide experimental exploration and interpretation.

III.B. Conformational Dependence in the CI UV-Visible Spectra of CH₃CHOO. In their aforementioned 2021 article on CH₂OO, McCoy, Marchetti, Thodika, and Karsili⁸⁸ also predicted UV-visible absorption spectra for the syn and anti conformers of CH₃CHOO (1 and 6, Scheme 1 above). As they found for CH2OO, McCoy et al.88 found that the CASPT2-(12,10)/aug-cc-pVDZ model chemistry outperformed MRCI-(10,8)+Q theory in predicting CH₃CHOO spectra that agree quite well with the experimental syn and anti spectra of Sheps et al. 98 and reasonably well with the *syn* spectrum of Smith et al. 99 and of Beames et al. 100 Based on EOM-CCSD/6-311++G(d,p) calculations, Beames et al. predicted that syn-CH3CHOO would be more destabilized by UV excitation than anti-CH3CHOO due to greater antibonding π^* interactions in the *B* state between the methyl group and the carbonyl oxide group in the syn conformer. Figure 1 provides a qualitative depiction of this argument.

The higher energy of the *B* state in *syn*-CH₃CHOO, coupled with the greater stability of ground-state *syn*-CH₃CHOO due to π stabilization between the methyl group and the terminal O,³⁷ can account qualitatively for the *syn*-CH₃CHOO absorption peak's being ~50 nm to the blue of the *anti*-CH₃CHOO absorption peak.⁹⁸ The relatively efficient nuclear ensemble method, coupled with the CASPT2(12,10)/aug-cc-pVDZ electronic structure method, successfully predicted the difference in the *syn* and *anti* UV–visible absorption peaks. It is also noteworthy that the same –0.7 eV shift that brought TDDFT and experimental UV–visible spectra for CH₂OO into agreement also successfully corrected the TDDFT spectra of *syn*- and *anti*-CH₃CHOO.

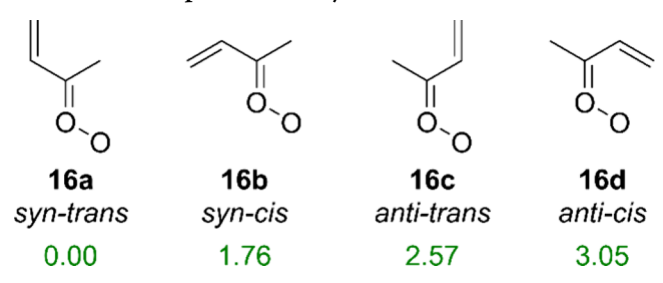
III.C. Predicted UV-Visible Spectra of Isoprene-**Derived Cls.** The presence of vinyl substituents in MVK oxide and MACR oxide makes the electronic excitation of these CIs more atmospherically relevant and theoretically richer. First, the presence of the vinyl groups shifts the $\pi^* \leftarrow \pi$ absorption of the carbonyl oxide moieties to longer wavelengths. 101 This increases the overlap of the CI absorption envelopes with the solar spectrum, making O-O photodissociation a potentially important limiter of CI atmospheric lifetime. 102 Second, the vinyl group doubles the number of MVK oxide and MACR oxide conformers compared to CH₃CHOO. Thus, there is the potential for the UV-visible spectra to reveal the presence of up to four conformers of each of the isoprene-derived CIs. Finally, the vinyl group orientation in the anti-methyl MVK oxide conformers (Scheme 4 above) and the syn-MACR oxide conformers (Scheme 5 above) makes possible the rapid formation of dioxoles^{39,46} and their subsequent decomposition, 44 thereby enhancing the contributions of syn-methyl MVK oxides and anti-MACR oxides to the observed UV-visible spectra.

With this context in mind, let us consider how Karsili and Nikoobakht modeled the UV-visible spectra of the four conformers of MVK oxide (Scheme 10).

In 2022, McCoy, Léger, Frey, Vansco, Marchetti, and Karsili (McCoy et al¹⁰²) computed vertical excitation energies and transition dipole moments for a Wigner distribution of geometries on the ground state potential energy surface; that is, the nuclear ensemble method. McCoy et al. computed the requisite electronic structure data with CASPT2(12,10) theory and the aug-cc-pVDZ basis set, as well as with TDDFT with the CAM-B3LYP functional and the 6-311+G(d,p) basis set. The 10

ı

Scheme 10. Four Conformers of Methyl Vinyl Ketone Oxide Produced in Isoprene Ozonolysis^a



"Relative energies (0 K, kcal mol⁻¹) as reported by Barber et al.³¹ based on a modified version of ANL0-F12 theory.⁴²

orbitals in the CASPT2 active space comprised the σ/σ^* and π/σ^* orbitals associated with the carbonyl oxide and vinyl groups. McCoy et al. also tested (10,8) and (8,6) active spaces.

The spectrum predicted for the *syn-trans* conformer of MVK oxide with CASPT2(12,10) theory agreed well with the $\lambda_{\rm max}$ values and widths of UV–visible spectra collected under two rather different experimental conditions: a 298-K sample measured via UV–visible direct absorption by Caravan et al. 32 ($\lambda_{\rm max}\approx 370$ nm) and a jet-cooled sample measured via depletion of the MVK oxide ion signal (at m/z=86) created by 118 nm vacuum-UV radiation by Vansco et al. 103 ($\lambda_{\rm max}\approx 390$ nm). The TDDFT *syn-trans* spectrum, shifted to the red by the same correction term (\sim 0.7 eV) found for CH₂OO and CH₃CHOO, 88 also agreed well with experiment. The *syn-trans* UV–visible spectra predicted with the smaller (10,8) and (8,6) active spaces were shifted 50–100 nm to the red of the experimental spectra, indicating the importance of a sufficiently large active space for quantitative accuracy.

large active space for quantitative accuracy.

The spectra predicted by McCoy et al. 102 for the other three MVK oxide conformers were all 50-100 nm to the red of that predicted for the syn-trans conformer and did not match the experimental spectra of Vansco et al. 103 and Caravan et al. 21 It is reasonable that in both experiments, the most abundant form of MVK oxide was the ground state syn-trans conformer. Based on the relative energies reported in Scheme 10, McCoy et al. predicted that at 250 K, 96% of MVK oxide would be in the syntrans form. Moreover, the relatively long lifetime of syn-trans (16a, Scheme 4 above) with respect to unimolecular reaction is consistent with its high relative abundance in the spectroscopy experiments. The Vansco et al. spectrum, with a peak ~20 nm to the red of the Caravan et al. spectrum, may reflect the presence of less stable MVK oxide conformers in the Vansco experiment. Significant populations of these conformers could have been generated during photolysis of the diiodoalkene precursor and "locked in" by the subsequent supersonic expansion, giving rise to a non-Boltzmann distribution of conformers.

I now consider the treatments of the MVK oxide UV—visible spectrum by Nikoobakht. $^{104-106}$ An initial study in 2022^{104} followed the same rigorous quantum dynamics approach taken in the 2021 CH₂OO study, 84 but the only electronic structure method used was EOM-CCSD/aug-cc-pVDZ. Nikoobakht's spectrum for the *syn-trans* conformer agreed best with the spectra measured by Vansco et al. 103 and Caravan et al.; 32 this conformer-specific agreement was consistent with the theoretical findings of McCoy et al. 102 Nikoobakht also predicted that all four conformers possess a strong avoided crossing between the B^1A' and C^1A' states, leading to barriers of 5.8-6.0 eV along the R(O-O) coordinate of the B state potential. As described above

for the Nikoobakht and Köppel $\mathrm{CH_2OO}$ spectrum, ⁸⁴ these barriers cause reflection of the wavepacket on the *B* potential, giving rise to vibrational progressions with peak spacings of ~ 0.07 eV. However, for the MVK oxide spectrum, the predicted vibrations were attributed to excitations of the C–O–O bending mode, not the O–O stretching mode. Neither the Vansco et al. nor the Caravan et al. spectrum exhibited any unambiguous vibrational structure.

Nikoobakht's subsequent 2023 study of MVK oxide 105,106 took the same quantum dynamics approach combined with the RS2C(12,10)/aug-cc-pVDZ model chemistry. (RS2C is, like CASPT2, a version of second-order multireference perturbation theory. 107) Nikoobakht's main argument for using a multireference electronic structure method, in contrast to EOM-CCSD, was the need for more accurate calculations of electronic energies at values of R(O-O) far from the equilibrium bond length in ground-state MVK oxide. Compared to the EOM-CCSD calculations, the RS2C(12,10) calculations predicted significant red shifts in each of the conformer-dependent spectra, from \sim 20 nm for anti-cis to \sim 70 nm for anti-trans. Overall, the RS2C(12,10) spectra of the syn-cis and syn-trans conformers agreed best with the experimental spectra of Vansco et al. 103 and Caravan et al. 32 as well as with a more recent roomtemperature UV-visible spectrum measured by Lin et al. 108 via depletion of MVK oxide absorption at 352 nm. The RS2C-(12,10) calculations also predicted pronounced vibrational structure for the spectra of all four conformers due to excitations of the O-O stretching and the C-O-O bending vibrations. These spectroscopic features are not evident in the experimental spectra reported to date. 32,103,108

Taking a step back, UV—visible spectroscopy with accurately measured absorption cross sections has the potential to be an effective way to quantify specific conformers of MVK oxide. ¹⁰³ Based on the locations of absorption maxima, according to the predictions of McCoy et al., ¹⁰² one could readily selectively detect the *syn-trans* and *anti-cis* conformers, while there is significant spectral overlap for *anti-trans* and *syn-cis*. In contrast, Nikoobakht ¹⁰⁵ predicted well-separated absorption maxima for the *anti-cis* and *anti-trans* conformers, with significant spectral overlap for *syn-cis* and *syn-trans*.

I next consider the UV-visible spectroscopy of the four conformers of MACR oxide (Scheme 11).

McCoy, Léger, Frey, Vansco, Marchetti, and Karsili (McCoy et al.) 102 applied the same methodology to MACR oxide as they applied to MVK oxide. Unlike the predicted UV–visible spectra for the MVK oxide conformers, the predicted spectra for the MACR oxide conformers overlapped considerably, with the $\lambda_{\rm max}$

Scheme 11. Four Conformers of Methacrolein Oxide Produced in Isoprene Ozonolysis^a

"Relative energies (0 K, kcal mol⁻¹) as reported by Vansco et al. 109 based on a modified version of ANL0-F12 theory. 42

values for the syn-cis, syn-trans, and anti-trans conformers all being \sim 400 nm; λ_{max} for the *anti-cis* conformer is \sim 440 nm. The predicted syn-cis, syn-trans, and anti-trans spectra all agreed reasonably well with the experimental UV-visible spectra recorded by Vansco et al. 109 (for a jet-cooled sample measured via depletion of MACR oxide ionized at 118 nm) and by Lin et al. 110 (for a thermalized sample at 298 K measured by direct absorption). Given the short lifetimes of the syn-MACR oxides with respect to dioxole formation (Scheme 5 above), it is reasonable to assume that the most abundant MACR oxide conformer in the Vansco and Lin experiments was anti-trans. One feature of the Vansco et al. spectrum that McCoy et al. could not capture was the weak oscillations, spaced by ~850 cm⁻¹, in the long-wavelength side of the absorption peak. Vansco et al. attributed the oscillations to vibrational resonances associated with the O-O stretching mode, among other normal modes, in the MACR oxide. It would be illuminating to model the MACR oxide UV-visible spectra with the quantum dynamics approach of Nikoobakht and see if the oscillation pattern can be replicated.

III.D. Predicted UV–Visible Spectra of Other Cls. While the combination of the Multi-Configuration Time Dependent Hartree (MCTDH) approach⁸⁵ to quantum dynamics and the RS2C electronic structure method did not provide the most accurate model of the MVK oxide UV–visible spectrum, this approach was quite successful in modeling the spectrum of 1-propanal oxide, CH₃CH₂CHOO (Scheme 12).

Scheme 12. Three Conformers of 1-Propanol Oxide^a

"Numbers in green are CBS-QB3 zero-point-corrected electronic energies (kcal mol⁻¹), all relative to the energy of **45a**, calculated for this article. In the stereochemical labels, *anti* and *gauche* characterize the relative orientation of the C–C and the C=O bonds.

In 2023, Nikoobakht and Köppel¹¹¹ reported theoretical spectra of both the more stable conformer of syn-CH₃CH₂CHOO (labeled as syn-anti in Scheme 12) and antigauche-CH₃CH₂CHOO. The predicted syn-CH₃CH₂CHOO spectrum agreed well with the experimental spectrum recorded by Liu et al. 10 via depletion of the CH₃CH₂CHOO as monitored by the intensity of parent ion which was generated by ionization at 118 nm. Observation of only syn-CH₃CH₂CHOO is consistent with its being the most stable conformer. Notably, neither the experimental nor the theoretical spectrum, treated with a dephasing time of 10 fs, had any oscillatory features. The predicted λ_{max} value for *syn-anti* is ~50 nm to the blue of the predicted λ_{max} value for anti-gauche, which is a manifestation of the same effect predicted for syn-CH3CHOO and anti-CH₃CHOO discussed above. It would be interesting to predict the UV-visible spectrum of the syn-gauche conformer and see if a convolution of the syn-anti and syn-gauche spectra agrees even better with the experimental spectrum.

I end by considering the UV-visible spectroscopy predicted by Wang, Liu, Zou, Sojdak, Kozlowski, Karsili, and Lester (Wang et al. 112) for the first $\pi^* \leftarrow \pi$ transition of the eight conformers of 2-butenal oxide (Scheme 6 above) using CASPT2(14,12)/augcc-pVDZ and the nuclear ensemble method. There is little variation with conformation in the spectra predicted for the four lowest-energy conformers: there is significant overlap among the four spectra and λ_{max} values range only from ~380 nm for the ground-state cZE conformer to \sim 420 nm for the tZE conformer. The experimental spectrum was of a jet-cooled sample measured via depletion of the 2-butenal oxide ion signal created by 118 nm vacuum-UV radiation. This spectrum had peaks at 343 and 373 nm; the absorbance dropped sharply at short wavelengths (the half-maximum absorbance was at ~320 nm), but extended significantly to the red of the 373 nm peak (the half-maximum absorbance was at ~420 nm). Overall, the spectrum predicted for the cZE conformer agreed best with the experimental spectrum for $\lambda > 350$ nm. The only conformer with a predicted first $\pi^* \leftarrow \pi$ vertical excitation energy to the blue of the *cZE* conformer was cZZ. The cZZ conformer could help account for the absorption local maximum at 343 nm; however, it is the least stable of the eight conformers and the one (Scheme 7 above) prone to a rapid unimolecular 1,6-hydrogen shift and subsequent decomposition. It may be instructive to repeat the experiment under different sets of source conditions; this would presumably generate different distributions of CI conformers and corresponding changes in the absorption spectrum.

In conclusion, we see that the UV—visible spectrum of Criegee intermediates has the potential to be a conformationally selective method for determining CI concentration. However, this selectivity naturally decreases as the number of conformations increases. The ability to assign spectral features is also contingent on the specific properties of the CI; for example, the predicted spectra of the four conformers of MVK oxide differ from one another significantly more than the spectra of the four conformers of MACR oxide. 102 It does not appear necessary to treat wavepacket dynamics to predict the main features of CI UV—visible spectra, but an explicit treatment of quantum effects is of course necessary to model spectra features such as vibrational progressions.

IV. CONCLUSIONS

Computation has played an essential role in delineating how the unimolecular and bimolecular reactions of small Criegee intermediates depend on CI conformation. In conjunction with state-of-the-art experimental measurements, computation has predicted that CIs with syn-alkyl groups typically undergo rapid 1,4-hydrogen shift reactions to form unstable vinyl hydroperoxides, CIs with syn-vinyl groups undergo very rapid cyclization reactions to form unstable dixoles, and other CIs react with water or sulfur dioxide faster than they cyclize to dioxiranes. Single-reference electronic structure methods applied to manually located conformers, conventional transition state theory, and the Eckart tunneling method have been sufficient to make predictions in excellent agreement with experiment. However, computational modeling of larger CIs that can make significant contributions to atmospheric aerosol formation will require use of automated conformational searching methods. Understanding how roaming mitigates OH production from VHPs will require electronic structure calculations that include treatments of both static and dynamic electron correlation as well as a variational treatment of loose transition states.

Electronic excitation, specifically the (first) $\pi^* \leftarrow \pi$ transition, and subsequent O–O photodissociation are atmospherically significant for the less reactive conformers of conjugated CIs. Whether or not an explict treatment of excited-state wavepacket dynamics is necessary depends on the desired resolution of the predicted UV–visible absorption spectrum. CASPT2 theory with large active spaces can generate accurate spectra even with only double- ζ basis sets. A combination of experiment and theory can be diagnostic for the presence of specific CI conformers if there is sufficient spectral difference among the individual conformers.

AUTHOR INFORMATION

Corresponding Author

Keith T. Kuwata — Department of Chemistry, Macalester College, Saint Paul, Minnesota 55105-1899, United States; orcid.org/0000-0002-3542-2081; Phone: (651) 696-6768; Email: kuwata@macalester.edu

Complete contact information is available at: https://pubs.acs.org/10.1021/acs.jpca.4c04517

Notes

The author declares no competing financial interest.



Keith T. Kuwata is a Professor of Chemistry at Macalester College, an undergraduate liberal arts institution in Saint Paul, Minnesota. He earned a bachelor's degree in chemistry from Harvey Mudd College in 1991, experiencing the joys and challenges of undergraduate research while working with Kerry K. Karukstis and G. William Daub. He then earned a Ph.D. in chemistry from the California Institute of Technology in 1998, working with Mitchio Okumura on questions of ion solvation and stratospheric ozone depletion. From 1998 to 2000, he served as a postdoctoral scholar at the University of California, Los Angeles, working with K. N. Houk and Suzanne E. Paulson on mechanisms of organic oxidation reactions in the troposphere. His research program at Macalester has focused on the use of quantum chemistry and statistical rate theory to predict atmospheric reaction mechanisms; his laboratory has also collaborated with a variety of experimentalists to interpret sometimes baffling results. Since starting a tenure-track position at Macalester in 2000, he has mentored 70 undergraduate research students and received support for his research from the American Chemical Society Petroleum Research Fund, the Camille and Henry Dreyfus Foundation, and the National Science Foundation. Highlights of his professional activities include cofounding and coleading the Midwest Undergraduate Computational Chemistry Consortium for the past 21 years, six years of service on the Petroleum Research Fund Committee, and nine years of service as chair of Macalester's Chemistry

Department. When not at work, he enjoys reading and talking about religion and politics, traveling, and relaxing with his family (his wife Alexa and their children Margaret, William, Jane, and Lydia) and friends.

ACKNOWLEDGMENTS

The author acknowledges support from the National Science Foundation (CHE-2108202) as well as access to the computational facilities of the Midwest Undergraduate Computational Chemistry Consortium at Hope College (established by NSF grants CHE-0520704, CHE-1039925, and OAC-1919571). The author thanks Macalester College undergraduate students Joseph B. Madell and Renee S. Nicholson for help with transition state theory calculations performed for this Perspective.

REFERENCES

- (1) Gutbrod, R.; Schindler, R. N.; Kraka, E.; Cremer, D. Formation of OH Radicals in the Gas Phase Ozonolysis of Alkenes: The Unexpected Role of Carbonyl Oxides. *Chem. Phys. Lett.* **1996**, *252*, 221–229.
- (2) Anglada, J. M.; Bofill, J. M.; Olivella, S.; Solé, A. Unimolecular Isomerizations and Oxygen Atom Loss in Formaldehyde and Acetaldehyde Carbonyl Oxides. A Theoretical Investigation. *J. Am. Chem. Soc.* **1996**, *118*, 4636–4647.
- (3) Olzmann, M.; Kraka, E.; Cremer, D.; Gutbrod, R.; Andersson, S. Energetics, Kinetics, and Product Distributions of the Reactions of Ozone with Ethene and 2,3-Dimethyl-2-Butene. *J. Phys. Chem. A* **1997**, 101, 9421–9429.
- (4) Cremer, D.; Kraka, E.; Szalay, P. G. Decomposition Modes of Dioxirane, Methyldioxirane and Dimethyldioxirane—a CCSD(T), MR-AQCC and DFT Investigation. *Chem. Phys. Lett.* **1998**, 292, 97–109.
- (5) Kroll, J. H.; Donahue, N. M.; Cee, V. J.; Demerjian, K. L.; Anderson, J. G. Gas-Phase Ozonolysis of Alkenes: Formation of OH from Anti Carbonyl Oxides. *J. Am. Chem. Soc.* **2002**, *124*, 8518–8519.
- (6) Nguyen, T. L.; Lee, H.; Matthews, D. A.; McCarthy, M. C.; Stanton, J. F. Stabilization of the Simplest Criegee Intermediate from the Reaction between Ozone and Ethylene: A High-Level Quantum Chemical and Kinetic Analysis of Ozonolysis. *J. Phys. Chem. A* **2015**, 119, 5524–5533.
- (7) Bomble, Y. J.; Vázquez, J.; Kállay, M.; Michauk, C.; Szalay, P. G.; Császár, A. G.; Gauss, J.; Stanton, J. F. High-accuracy Extrapolated Ab Initio Thermochemistry. II. Minor Improvements to the Protocol and a Vital Simplification. *J. Chem. Phys.* **2006**, *125*, No. 064108.
- (8) Wennberg, P. O. Atmospheric Chemistry: Radicals Follow the Sun. *Nature* **2006**, 442, 145–146.
- (9) Liu, F.; Beames, J. M.; Petit, A. S.; McCoy, A. B.; Lester, M. I. Infrared-Driven Unimolecular Reaction of CH₃CHOO Criegee Intermediates to OH Radical Products. *Science* **2014**, 345, 1596–1598.
- (10) Liu, F.; Beames, J. M.; Green, A. M.; Lester, M. I. UV Spectroscopic Characterization of Dimethyl- and Ethyl-Substituted Carbonyl Oxides. *J. Phys. Chem. A* **2014**, *118*, 2298–2306.
- (11) Lu, L.; Beames, J. M.; Lester, M. I. Early Time Detection of OH Radical Products from Energized Criegee Intermediates CH₂OO and CH₃CHOO. *Chem. Phys. Lett.* **2014**, *598*, 23.
- (12) Fang, Y.; Liu, F.; Barber, V. P.; Klippenstein, S. J.; McCoy, A. B.; Lester, M. I. Real Time Observation of Unimolecular Decay of Criegee Intermediates to OH Radical Products. *J. Chem. Phys.* **2016**, *144*, No. 061102.
- (13) Fang, Y.; Liu, F.; Klippenstein, S. J.; Lester, M. I. Direct Observation of Unimolecular Decay of CH₃CH₂CHOO Criegee Intermediates to OH Radical Products. *J. Chem. Phys.* **2016**, *145*, No. 044312.
- (14) Kroll, J. H.; Sahay, S. R.; Anderson, J. G.; Demerjian, K. L.; Donahue, N. M. Mechanism of HO_x Formation in the Gas-Phase Ozone-Alkene Reaction. 2. Prompt versus Thermal Dissociation of Carbonyl Oxides to Form OH. *J. Phys. Chem. A* **2001**, *105*, 4446–4457.

- (15) Aplincourt, P.; Ruiz-López, M. F. Theoretical Investigation of Reaction Mechanisms for Carboxylic Acid Formation in the Atmosphere. J. Am. Chem. Soc. 2000, 122, 8990–8997.
- (16) Crehuet, R.; Anglada, J. M.; Bofill, J. M. Tropospheric Formation of Hydroxymethyl Hydroperoxide, Formic Acid, H_2O_2 , and OH from Carbonyl Oxide in the Presence of Water Vapor: A Theoretical Study of the Reaction Mechanism. *Chemistry A European Journal* **2001**, *7*, 2227–2235.
- (17) Aplincourt, P.; Anglada, J. M. Theoretical Studies on Isoprene Ozonolysis under Tropospheric Conditions. 1. Reactions of Substituted Carbonyl Oxides with Water. *J. Phys. Chem. A* **2003**, *107*, 5798–5811.
- (18) Cox, R. A.; Penkett, S. A. Oxidation of Atmospheric SO₂ by Products of the Ozone-Olefin Reaction. *Nature* **1971**, 230, 321–322.
- (19) Mauldin, R. L., III; Berndt, T.; Sipilä, M.; Paasonen, P.; Petaja, T.; Kim, S.; Kurtén, T.; Stratmann, F.; Kerminen, V.-M.; Kulmala, M. A New Atmospherically Relevant Oxidant of Sulphur Dioxide. *Nature* **2012**, *488*, 193–196.
- (20) Welz, O.; Savee, J. D.; Osborn, D. L.; Vasu, S. S.; Percival, C. J.; Shallcross, D. E.; Taatjes, C. A. Direct Kinetic Measurements of Criegee Intermediate (CH₂OO) Formed by Reaction of CH₂I with O₂. *Science* **2012**, 335, 204–207.
- (21) Chhantyal-Pun, R.; Davey, A.; Shallcross, D. E.; Percival, C. J.; Orr-Ewing, A. J. A Kinetic Study of the CH₂OO Criegee Intermediate Self-Reaction, Reaction with SO₂ and Unimolecular Reaction using Cavity Ring-Down Spectroscopy. *Phys. Chem. Chem. Phys.* **2015**, *17*, 3617–3626.
- (22) Hasson, A. S.; Chung, M. Y.; Kuwata, K. T.; Converse, A. D.; Krohn, D.; Paulson, S. E. Reaction of Criegee Intermediates with Water Vapor-An Additional Source of OH Radicals in Alkene Ozonolysis? *J. Phys. Chem. A* **2003**, *107*, 6176–6182.
- (23) Cox, R. A.; Ammann, M.; Crowley, J. N.; Herrmann, H.; Jenkin, M. E.; McNeill, V. F.; Mellouki, A.; Troe, J.; Wallington, T. J. Evaluated Kinetic and Photochemical Data for Atmospheric Chemistry: Volume VII Criegee Intermediates. *Atmos. Chem. Phys.* **2020**, *20*, 13497—13519.
- (24) Kuwata, K. T.; Hermes, M. R.; Carlson, M. J.; Zogg, C. K. Computational Studies of the Isomerization and Hydration Reactions of Acetaldehyde Oxide and Methyl Vinyl Carbonyl Oxide. *J. Phys. Chem. A* **2010**, *114*, 9192–9204.
- (25) Taatjes, C. A.; Welz, O.; Eskola, A. J.; Savee, J. D.; Scheer, A. M.; Shallcross, D. E.; Rotavera, B.; Lee, E. P. F.; Dyke, J. M.; Mok, D. K. W.; Osborn, D. L.; Percival, C. J. Direct Measurements of Conformer-Dependent Reactivity of the Criegee Intermediate CH₃CHOO. *Science* **2013**, 340, 177–180.
- (26) Novelli, A.; Vereecken, L.; Lelieveld, J.; Harder, H. Direct Observation of OH Formation from Stabilised Criegee Intermediates. *Phys. Chem. Phys.* **2014**, *16*, 19941–19951.
- (27) Long, B.; Bao, J. L.; Truhlar, D. G. Atmospheric Chemistry of Criegee Intermediates: Unimolecular Reactions and Reactions with Water. J. Am. Chem. Soc. 2016, 138, 14409–14422.
- (28) Robinson, C.; Onel, L.; Newman, J.; Lade, R.; Au, K.; Sheps, L.; Heard, D. E.; Seakins, P. W.; Blitz, M. A.; Stone, D. Unimolecular Kinetics of Stabilized CH₃CHOO Criegee Intermediates: syn-CH₃CHOO Decomposition and anti-CH₃CHOO Isomerization. *J. Phys. Chem. A* **2022**, *126*, 6984–6994.
- (29) Glowacki, D. R.; Liang, C.-H.; Morley, C.; Pilling, M. J.; Robertson, S. H. MESMER: An Open-Source Master Equation Solver for Multi-Energy Well Reactions. *J. Phys. Chem. A* **2012**, *116*, 9545–9560
- (30) Vereecken, L.; Novelli, A.; Taraborrelli, D. Unimolecular Decay Strongly Limits the Atmospheric Impact of Criegee Intermediates. *Phys. Chem. Chem. Phys.* **2017**, *19*, 31599–31612.
- (31) Barber, V. P.; Pandit, S.; Green, A. M.; Trongsiriwat, N.; Walsh, P. J.; Klippenstein, S. J.; Lester, M. I. Four-Carbon Criegee Intermediate from Isoprene Ozonolysis: Methyl Vinyl Ketone Oxide Synthesis, Infrared Spectrum, and OH Production. *J. Am. Chem. Soc.* **2018**, *140*, 10866–10880.

- (32) Caravan, R. L.; Vansco, M. F.; Au, K.; Khan, M. A. H.; Li, Y.-L.; Winiberg, F. A. F.; Zuraski, K.; Lin, Y.-H.; Chao, W.; Trongsiriwat, N.; Walsh, P. J.; Osborn, D. L.; Percival, C. J.; Lin, J. J.-M.; Shallcross, D. E.; Sheps, L.; Klippenstein, S. J.; Taatjes, C. A.; Lester, M. I. Direct Kinetic Measurements and Theoretical Predictions of an Isoprene-derived Criegee Intermediate. *Proc. Natl. Acad. Sci. U. S. A.* **2020**, *117*, 9733—9740
- (33) Anglada, J. M.; Aplincourt, P.; Bofill, J. M.; Cremer, D. Atmospheric Formation of OH Radicals and H₂O₂ from Alkene Ozonolysis under Humid Conditions. *ChemPhysChem* **2002**, *3*, 215–221
- (34) Ryzhkov, A. B.; Ariya, P. A. A Theoretical Study of the Reactions of Parent and Substituted Criegee Intermediates with Water and the Water Dimer. *Phys. Chem. Chem. Phys.* **2004**, *6*, 5042–5050.
- (35) Anglada, J. M.; González, J.; Torrent-Sucarrat, M. Effects of the Substituents on the Reactivity of Carbonyl Oxides. A Theoretical Study on the Reaction of Substituted Carbonyl Oxides with Water. *Phys. Chem. Chem. Phys.* **2011**, *13*, 13034–13045.
- (36) Lynch, B. J.; Truhlar, D. G. Robust and Affordable Multi-coefficient Methods for Thermochemistry and Thermochemical Kinetics: The MCCM/3 Suite and SAC/3. *J. Phys. Chem. A* **2003**, 107, 3898–3906.
- (37) Cremer, D. Theoretical Determination of Molecular Structure and Conformation. 6. The Criegee Intermediate. Evidence for a Stabilization of Its Syn Form by Alkyl Substituents. *J. Am. Chem. Soc.* **1979**, *101*, 7199–7205.
- (38) Guha, S. K.; Shibayama, A.; Abe, D.; Sakaguchi, M.; Ukaji, Y.; Inomata, K. Syn-Effect" in the Conversion of (E)- α , β -Unsaturated Esters into the Corresponding β , γ -Unsaturated Esters and Aldehydes into Silyl Enol Ethers. *Bull. Chem. Soc. Jpn.* **2004**, *77*, 2147–2157.
- (39) Kuwata, K. T.; Valin, L. C.; Converse, A. D. Quantum Chemical and Master Equation Studies of the Methyl Vinyl Carbonyl Oxides Formed in Isoprene Ozonolysis. *J. Phys. Chem. A* **2005**, *109*, 10710–10725.
- (40) Barker, J. R. Multiple-Well, Multiple-Path Unimolecular Reaction Systems. I. MultiWell Computer Program Suite. *Int. J. Chem. Kinet.* **2001**, 33, 232–245.
- (41) Barker, J. R. MultiWell-1.3.3; Oct 2003.
- (42) Klippenstein, S. J.; Harding, L. B.; Ruscic, B. Ab Initio Computations and Active Thermochemical Tables Hand in Hand: Heats of Formation of Core Combustion Species. *J. Phys. Chem. A* **2017**, *121*, 6580–6602.
- (43) Osborn, D. L.; Zou, P.; Johnsen, H.; Hayden, C. C.; Taatjes, C. A.; Knyazev, V. D.; North, S. W.; Peterka, D. S.; Ahmed, M.; Leone, S. R. The Multiplexed Chemical Kinetic Photoionization Mass Spectrometer: A New Approach to Isomer-resolved Chemical Kinetics. *Rev. Sci. Instrum.* **2008**, *79*, No. 104103.
- (44) Vansco, M. F.; Caravan, R. L.; Zuraski, K.; Winiberg, F. A. F.; Au, K.; Trongsiriwat, N.; Walsh, P. J.; Osborn, D. L.; Percival, C. J.; Khan, M. A. H.; Shallcross, D. E.; Taatjes, C. A.; Lester, M. I. Experimental Evidence of Dioxole Unimolecular Decay Pathway for Isoprene-Derived Criegee Intermediates. *J. Phys. Chem. A* **2020**, *124*, 3542–3554.
- (45) Eckart, C. The Penetration of a Potential Barrier by Electrons. *Phys. Rev.* **1930**, *35*, 1303–1309.
- (46) Kuwata, K. T.; Valin, L. C. Quantum Chemical and RRKM/Master Equation Studies of Isoprene Ozonolysis: Methacrolein and Methacrolein Oxide. *Chem. Phys. Lett.* **2008**, *451*, 186–191.
- (47) Hansen, A. S.; Qian, Y.; Sojdak, C. A.; Kozlowski, M. C.; Esposito, V. J.; Francisco, J. S.; Klippenstein, S. J.; Lester, M. I. Rapid Allylic 1,6 H-Atom Transfer in an Unsaturated Criegee Intermediate. *J. Am. Chem. Soc.* **2022**, *144*, 5945–5955.
- (48) Vereecken, L.; Novelli, A.; Kiendler-Scharr, A.; Wahner, A. Unimolecular and Water Reactions of Oxygenated and Unsaturated Criegee Intermediates under Atmospheric Conditions. *Phys. Chem. Chem. Phys.* **2022**, *24*, 6428–6443.
- (49) Dorigo, A. E.; Houk, K. N. Transition Structures for Intramolecular Hydrogen-atom Transfers: The Energetic Advantage

- of Seven-membered over Six-membered Transition Structures. J. Am. Chem. Soc. 1987, 109, 2195–2197.
- (50) Georgievskii, Y.; Klippenstein, S. J. MESS Master Equation System Solver; 2020.1.24; Argonne National Laboratory: 2020.
- (51) Sindelarova, K.; Granier, C.; Bouarar, I.; Guenther, A.; Tilmes, S.; Stavrakou, T.; Müller, J. F.; Kuhn, U.; Stefani, P.; Knorr, W. Global Data Set of Biogenic VOC Emissions Calculated by the MEGAN Model over the Last 30 Years. *Atmos. Chem. Phys.* **2014**, *14*, 9317–9341.
- (52) Utembe, S. R.; Cooke, M. Ć.; Archibald, A. T.; Jenkin, M. E.; Derwent, R. G.; Shallcross, D. E. Using a Reduced Common Representative Intermediates (CRIv2-R5) Mechanism to Simulate Tropospheric Ozone in a 3-D Lagrangian Chemistry Transport Model. *Atmos. Environ.* **2010**, *44*, 1609–1622.
- (53) Ziemann, P. J.; Atkinson, R. Kinetics, Products, and Mechanisms of Secondary Organic Aerosol Formation. *Chem. Soc. Rev.* **2012**, *41*, 6582–6605.
- (54) Seinfeld, J. H.; Bretherton, C.; Carslaw, K. S.; Coe, H.; DeMott, P. J.; Dunlea, E. J.; Feingold, G.; Ghan, S.; Guenther, A. B.; Kahn, R.; Kraucunas, I.; Kreidenweis, S. M.; Molina, M. J.; Nenes, A.; Penner, J. E.; Prather, K. A.; Ramanathan, V.; Ramaswamy, V.; Rasch, P. J.; Ravishankara, A. R.; Rosenfeld, D.; Stephens, G.; Wood, R. Improving our Fundamental Understanding of the Role of Aerosol-cloud Interactions in the Climate System. *Proc. Natl. Acad. Sci. U. S. A.* **2016**, *113*, 5781–5790.
- (55) Silva, R. A.; West, J. J.; Zhang, Y. Q.; Anenberg, S. C.; Lamarque, J. F.; Shindell, D. T.; Collins, W. J.; Dalsoren, S.; Faluvegi, G.; Folberth, G.; Horowitz, L. W.; Nagashima, T.; Naik, V.; Rumbold, S.; Skeie, R.; Sudo, K.; Takemura, T.; Bergmann, D.; Cameron-Smith, P.; Cionni, I.; Doherty, R. M.; Eyring, V.; Josse, B.; MacKenzie, I. A.; Plummer, D.; Righi, M.; Stevenson, D. S.; Strode, S.; Szopa, S.; Zeng, G. Global Premature Mortality Due to Anthropogenic Outdoor Air Pollution and the Contribution of Past Climate Change. *Environmental Research Letters* **2013**, *8*, No. 034005.
- (56) Spartan'24; Wavefunction, Inc.: Irvine, CA.
- (57) Pracht, P.; Bohle, F.; Grimme, S. Automated Exploration of the Low-energy Chemical Space with Fast Quantum Chemical Methods. *Phys. Chem. Chem. Phys.* **2020**, 22, 7169–7192.
- (58) Bannwarth, C.; Ehlert, S.; Grimme, S. GFN2-xTB—An Accurate and Broadly Parametrized Self-Consistent Tight-Binding Quantum Chemical Method with Multipole Electrostatics and Density-Dependent Dispersion Contributions. *J. Chem. Theory Comput.* **2019**, *15*, 1652–1671.
- (59) Iyer, S.; Rissanen, M. P.; Valiev, R.; Barua, S.; Krechmer, J. E.; Thornton, J.; Ehn, M.; Kurtén, T. Molecular Mechanism for Rapid Autoxidation in α-Pinene Ozonolysis. *Nat. Commun.* **2021**, *12*, 878.
- (60) Pasik, D.; Frandsen, B. N.; Meder, M.; Iyer, S.; Kurtén, T.; Myllys, N. Gas-Phase Oxidation of Atmospherically Relevant Unsaturated Hydrocarbons by Acyl Peroxy Radicals. *J. Am. Chem. Soc.* **2024**, *146*, 13427–13437.
- (61) Story, P. R.; Burgess, J. R. Ozonolysis. Evidence for Carbonyl Oxide Tautomerization and for 1,3-Dipolar Addition to Olefins. *J. Am. Chem. Soc.* **1967**, *89*, 5726–5727.
- (62) Hull, L. A. Terpene Ozonolysis Products. In *Atmospheric Biogenic Hydrocarbons*; Bufalini, J. J.; Arnts, R. R., Eds.; Ann Arbor Science Publishers: Ann Arbor, MI, 1981; Vol. 2, pp 161–186.
- (63) Niki, H.; Maker, P. D.; Savage, C. M.; Breitenbach, L. P.; Hurley, M. D. FTIR Spectroscopic Study of the Mechanism for the Gas-Phase Reaction between Ozone and Tetramethylethylene. *J. Phys. Chem.* 1987, 91, 941–946.
- (64) Grosjean, E.; Grosjean, D. The Gas-Phase Reaction of Alkenes with Ozone: Formation Yields of Carbonyls from Biradicals in Ozone-Alkene-Cyclohexane Experiments. *Atmos. Environ.* **1998**, 32, 3393–3402
- (65) Taatjes, C. A.; Liu, F.; Rotavera, B.; Kumar, M.; Caravan, R.; Osborn, D. L.; Thompson, W. H.; Lester, M. I. Hydroxyacetone Production From C₃ Criegee Intermediates. *J. Phys. Chem. A* **2017**, *121*, 16–23.

- (66) Kurtén, T.; Donahue, N. M. MRCISD Studies of the Dissociation of Vinylhydroperoxide, CH₂CHOOH: There Is a Saddle Point. *J. Phys. Chem. A* **2012**, *116*, 6823–6830.
- (67) Kidwell, N. M.; Li, H.; Wang, X.; Bowman, J. M.; Lester, M. I. Unimolecular Dissociation Dynamics of Vibrationally Activated CH₃CHOO Criegee Intermediates to OH Radical Products. *Nat. Chem.* **2016**, *8*, 509–514.
- (68) Kuwata, K. T.; Luu, L.; Weberg, A. B.; Huang, K.; Parsons, A. J.; Peebles, L. A.; Rackstraw, N. B.; Kim, M. J. Quantum Chemical and Statistical Rate Theory Studies of the Vinyl Hydroperoxides Formed in *trans*-2-Butene and 2,3-Dimethyl-2-butene Ozonolysis. *J. Phys. Chem. A* 2018, 122, 2485–2502.
- (69) Levchenko, S. V.; Krylov, A. I. Equation-of-Motion Spin-Flip Coupled-Cluster Model with Single and Double Substitutions: Theory and Application to Cyclobutadiene. *J. Chem. Phys.* **2004**, *120*, 175–185.
- (70) Manohar, P. U.; Krylov, A. I. A Noniterative Perturbative Triples Correction for the Spin-Flipping and Spin-Conserving Equation-of-Motion Coupled-Cluster Methods with Single and Double Substitutions. J. Chem. Phys. 2008, 129, No. 194105.
- (71) Barnes, E. C.; Petersson, G. A.; Montgomery, J. A.; Frisch, M. J.; Martin, J. M. L. Unrestricted Coupled Cluster and Brueckner Doubles Variations of W1 Theory. *J. Chem. Theory Comput.* **2009**, *5*, 2687–2693.
- (72) Suits, A. G., Roaming Reactions and Dynamics in the van der Waals Region. In *Annual Review of Physical Chemistry*; Johnson, M. A., Martinez, T. J., Eds. **2020**; Vol. 71, pp 77–100.
- (73) Klippenstein, S. J.; Georgievskii, Y.; Harding, L. B. Statistical Theory for the Kinetics and Dynamics of Roaming Reactions. *J. Phys. Chem. A* **2011**, *115*, 14370–14381.
- (74) Barker, J. R.; Ortiz, N. F.; Preses, J. M.; Lohr, L. L.; Maranzana, A.; Stimac, P. J.; Nguyen, T. L.; Kumar, T. J. D. *MultiWell-2014.1*; University of Michigan: Ann Arbor, MI, June 2014.
- (75) Liu, T. L.; Elliott, S. N.; Zou, M. J.; Vansco, M. F.; Sojdak, C. A.; Markus, C. R.; Almeida, R.; Au, K. D.; Sheps, L.; Osborn, D. L.; Winiberg, F. A. F.; Percival, C. J.; Taatjes, C. A.; Caravan, R. L.; Klippenstein, S. J.; Lester, M. I. OH Roaming and Beyond in the Unimolecular Decay of the Methyl-Ethyl-Substituted Criegee Intermediate: Observations and Predictions. J. Am. Chem. Soc. 2023, 145, 19405–19420.
- (76) Liu, T. L.; Elliott, S. N.; Zou, M. J.; Vansco, M. F.; Sojdak, C. A.; Markus, C. R.; Almeida, R.; Au, K. D.; Sheps, L.; Osborn, D. L.; Winiberg, F. A. F.; Percival, C. J.; Taatjes, C. A.; Caravan, R. L.; Klippenstein, S. J.; Lester, M. I. OH Roaming and Beyond in the Unimolecular Decay of the Methyl-Ethyl-Substituted Criegee Intermediate: Observations and Predictions. *J. Am. Chem. Soc.* 2023, 145, 19405—19420.
- (77) Klippenstein, S. J.; Elliott, S. N. OH Roaming during the Ozonolysis of α -Pinene: A New Route to Highly Oxygenated Molecules? *J. Phys. Chem. A* **2023**, *127*, 10647–10662.
- (78) Pfeifle, M.; Ma, Y.-T.; Jasper, A. W.; Harding, L. B.; Hase, W. L.; Klippenstein, S. J. Nascent Energy Distribution of the Criegee Intermediate CH₂OO from Direct Dynamics Calculations of Primary Ozonide Dissociation. *J. Chem. Phys.* **2018**, *148*, No. 174306.
- (79) Klippenstein, S. J. Variational Optimizations in the Rice–Ramsperger–Kassel–Marcus Theory Calculations for Unimolecular Dissociations with No Reverse Barrier. *J. Chem. Phys.* **1992**, *96*, 367–371
- (80) Georgievskii, Y.; Klippenstein, S. J. Transition State Theory for Multichannel Addition Reactions: Multifaceted Dividing Surfaces. *J. Phys. Chem. A* **2003**, *107*, 9776–9781.
- (81) Yang, L.; Sonk, J. A.; Barker, J. R. HO + OClO Reaction System: Featuring a Barrierless Entrance Channel with Two Transition States. *J. Phys. Chem. A* **2015**, *119*, 5723–5731.
- (82) Barker, J. R.; Nguyen, T. L.; Stanton, J. F.; Aieta, C.; Ceotto, M.; Gabas, F.; Kumar, T. J. D.; Li, C. G. L.; Lohr, L. L.; Maranzana, A.; Ortiz, N. F.; Preses, J. M.; Simmie, J. M.; Sonk, J. A.; Stimac, P. J. *MultiWell-2023 Software Suite*; University of Michigan: Ann Arbor, MI, 2023.

- (83) Aplincourt, P.; Henon, E.; Bohr, F.; Ruiz-López, M. F. Theoretical Study of Photochemical Processes Involving Singlet Excited States of Formaldehyde Carbonyl Oxide in the Atmosphere. *Chem. Phys.* **2002**, 285, 221–231.
- (84) Nikoobakht, B.; Köppel, H. UV Absorption Spectrum and Photodissociation Dynamics of CH₂OO Following Excitation to the B¹A' State. *Mol. Phys.* **2021**, *119*, No. e1958019.
- (85) Meyer, H. D.; Manthe, U.; Cederbaum, L. S. The Multiconfigurational Time-dependent Hartree Approach. *Chem. Phys. Lett.* **1990**, *165*, 73–78.
- (86) Nikoobakht, B.; Köppel, H. Correlated Quantum Treatment of the Photodissociation Dynamics of Formaldehyde Oxide CH₂OO. *Phys. Chem. Chem. Phys.* **2022**, *24*, 12433–12441.
- (87) Shiozaki, T.; Werner, H.-J. Communication: Second-order Multireference Perturbation Theory with Explicit Correlation: CASPT2-F12. J. Chem. Phys. 2010, 133, No. 141103.
- (88) McCoy, J. C.; Marchetti, B.; Thodika, M.; Karsili, T. N. V. A Simple and Efficient Method for Simulating the Electronic Absorption Spectra of Criegee Intermediates: Benchmarking on CH₂OO and CH₃CHOO. *J. Phys. Chem. A* **2021**, *125*, 4089–4097.
- (89) Crespo-Otero, R.; Barbatti, M. Spectrum Simulation and Decomposition with Nuclear Ensemble: Formal Derivation and Application to Benzene, Furan and 2-Phenylfuran. *Theor. Chem. Acc.* **2012**, *131*, 1237.
- (90) Beames, J. M.; Liu, F.; Lu, L.; Lester, M. I. Ultraviolet Spectrum and Photochemistry of the Simplest Criegee Intermediate CH₂OO. *J. Am. Chem. Soc.* **2012**, *134*, 20045–20048.
- (91) Sheps, L. Absolute Ultraviolet Absorption Spectrum of a Criegee Intermediate CH₂OO. *J. Phys. Chem. Lett.* **2013**, *4*, 4201–4205.
- (92) Ting, W.-L.; Chen, Y.-H.; Chao, W.; Smith, M. C.; Lin, J. J.-M. The UV Absorption Spectrum of the Simplest Criegee Intermediate CH₂OO. *Phys. Chem. Chem. Phys.* **2014**, *16*, 10438–10443.
- (93) Foreman, E. S.; Kapnas, K. M.; Jou, Y.; Kalinowski, J.; Feng, D.; Gerber, R. B.; Murray, C. High Resolution Absolute Absorption Cross Sections of the B¹A'-X¹A' Transition of the CH₂OO Biradical. *Phys. Chem. Chem. Phys.* **2015**, *17*, 32539–32546.
- (94) Dawes, R.; Jiang, B.; Guo, H. UV Absorption Spectrum and Photodissociation Channels of the Simplest Criegee Intermediate (CH₂OO). *J. Am. Chem. Soc.* **2015**, *137*, 50–53.
- (95) Heller, E. J. Quantum Corrections to Classical Photodissociation Models. *J. Chem. Phys.* **1978**, *68*, 2066–2075.
- (96) Abrams, M. L.; Sherrill, C. D. An Assessment of the Accuracy of Multireference Configuration Interaction (MRCI) and Complete-Active-Space Second-Order Perturbation Theory (CASPT2) for Breaking Bonds to Hydrogen. J. Phys. Chem. A 2003, 107, 5611–5616. (97) Takahashi, K. Wave Packet Calculation of Absolute UV Cross
- (97) Takahashi, K. Wave Packet Calculation of Absolute UV Cross Section of Criegee Intermediates. *J. Phys. Chem. A* **2022**, 126, 6080–6090.
- (98) Sheps, L.; Scully, A. M.; Au, K. UV Absorption Probing of the Conformer-dependent Reactivity of a Criegee Intermediate CH₃CHOO. *Phys. Chem. Chem. Phys.* **2014**, *16*, 26701–26706.
- (99) Smith, M. C.; Ting, W.-L.; Chang, C.-H.; Takahashi, K.; Boering, K. A.; Lin, J. J.-M. UV Absorption Spectrum of the $\rm C_2$ Criegee Intermediate CH₃CHOO. *J. Chem. Phys.* **2014**, *141*, 074302.
- (100) Beames, J. M.; Liu, F.; Lu, L.; Lester, M. I. UV Spectroscopic Characterization of an Alkyl Substituted Criegee Intermediate CH₃CHOO. *J. Chem. Phys.* **2013**, *138*, No. 244307.
- (101) Yin, C.; Takahashi, K. How Big is the Substituent Dependence of the Solar Photolysis Rate of Criegee Intermediates? *Phys. Chem. Chem. Phys.* **2018**, *20*, 16247–16255.
- (102) McCoy, J. C.; Léger, S. J.; Frey, C. F.; Vansco, M. F.; Marchetti, B.; Karsili, T. N. V. Modeling the Conformer-Dependent Electronic Absorption Spectra and Photolysis Rates of Methyl Vinyl Ketone Oxide and Methacrolein Oxide. *J. Phys. Chem. A* **2022**, *126*, 485–496.
- (103) Vansco, M. F.; Marchetti, B.; Lester, M. I. Electronic Spectroscopy of Methyl Vinyl Ketone Oxide: A Four-carbon Unsaturated Criegee Intermediate from Isoprene Ozonolysis. *J. Chem. Phys.* **2018**, *149*, 244309.

- (104) Nikoobakht, B. An Ab Initio Quantum Dynamics Simulation of UV Absorption Spectrum of Methyl Vinyl Kene Oxide. *J. Chem. Phys.* **2022**, *157*, No. 014101.
- (105) Nikoobakht, B. UV Absorption Spectroscopy of the Conformer-Dependent Reactivity of the Four Carbon Criegee Intermediate of Methyl Vinyl Ketone Oxide: An Ab initio Quantum Dynamics Study. *J. Phys. Chem. A* **2023**, *127*, 10091–10103.
- (106) Nikoobakht, B. Correction to "UV Absorption Spectroscopy of the Conformer-Dependent Reactivity of the Four Carbon Criegee Intermediate of Methyl Vinyl Ketone Oxide: An Ab Initio Quantum Dynamics Study. *J. Phys. Chem. A* **2024**, *128*, 1972–1972.
- (107) Celani, P.; Werner, H.-J. Multireference Perturbation Theory for Large Restricted and Selected Active Space Reference Wave Functions. *J. Chem. Phys.* **2000**, *112*, 5546–5557.
- (108) Lin, Y.-H.; Takahashi, K.; Lin, J. J.-M. Absolute Photodissociation Cross Sections of Thermalized Methyl Vinyl Ketone Oxide and Methacrolein Oxide. *Phys. Chem. Chem. Phys.* **2022**, *24*, 10439– 10450.
- (109) Vansco, M. F.; Marchetti, B.; Trongsiriwat, N.; Bhagde, T.; Wang, G.; Walsh, P. J.; Klippenstein, S. J.; Lester, M. I. Synthesis, Electronic Spectroscopy, and Photochemistry of Methacrolein Oxide: A Four-Carbon Unsaturated Criegee Intermediate from Isoprene Ozonolysis. J. Am. Chem. Soc. 2019, 141, 15058–15069.
- (110) Lin, Y.-H.; Yin, C.; Takahashi, K.; Lin, J. J.-M. Surprisingly Long Lifetime of Methacrolein Oxide, an Isoprene Derived Criegee Intermediate, under Humid Conditions. *Commun. Chem.* **2021**, *4*, 12.
- (111) Nikoobakht, B.; Köppel, H. Conformational Dependence of the UV Absorption Spectrum of CH₃CH₂CHOO Following Excitation to the B¹A' State. *Chem. Phys. Lett.* **2023**, 833, No. 140943.
- (112) Wang, G.; Liu, T.; Zou, M.; Sojdak, C. A.; Kozlowski, M. C.; Karsili, T. N. V.; Lester, M. I. Electronic Spectroscopy and Dissociation Dynamics of Vinyl-Substituted Criegee Intermediates: 2-Butenal Oxide and Comparison with Methyl Vinyl Ketone Oxide and Methacrolein Oxide Isomers. *J. Phys. Chem. A* **2023**, 127, 203–215.